Few-Body Bound States of Dark Matter

by

Alexander F. Shaw

A thesis submitted in partial fulfillment of the requirements
for graduation with Honors in Physics.

Whitman College
2019

Certificate of Approval

This is to certify that the accompanying thesis by Alexander Francis Shaw has been accepted in partial fulfillment of the requirements for graduation with Honors in Physics.

Moira I. Gresham, Ph.D.

Whitman College
May 8th, 2019

Contents

1 Introduction

1.1 Asymmetric Dark Matter 4

1.2 Overview 6

2 The Two-Body Problem **9**

2.1 Determining the Two-Body Ground State 9

2.2 Yukawa Potential 11

2.3 Two Body Results and Discussion 13

3 The Few-Body Problem **17**

3.1 Introduction to the Quantum Few-Body Problem 17

3.2 Methods of Solving the Quantum Few-Body Problem 20

3.3 Introduction to the Stochastic Variational Method 21

3.4 Basis Vectors and Matrix Elements 24

3.5 Indistinguishable Particles 28

3.6 Exchange Interaction 31

3.7 Symmetrization 33

3.8 Application to ps^- 37

4 Results and Discussion **41**

5 Conclusion **48**

A Ritz Variational Method **51**

Abstract

Certain dark matter theories predict self interaction between dark matter particles. Assuming that dark matter particles interact pairwise via an attractive Yukawa potential, this analysis determines whether decay modes exist for three- and four-body bound states. These original results are reported in terms of the potential's screening length. Few-body calculations employ the Stochastic Variational Method of [1]. Accessible to an undergraduate audience, this work also discusses the relevant theory needed to apply this method and why the results are significant in dark matter research.

Acknowledgements

I am grateful to my adviser, Professor Moira Gresham, for her guidance and support both during this project and throughout my entire college career. I also want to thank the National Science Foundation for funding a summer of research that contributed to this thesis.

List of Figures

1.1 The Bullet Cluster 2

1.2 Galactic Rotation Curves 3

2.1 The Yukawa Potential 13

2.2 Two-Body Ground State Energy and Radial Probability Distributions 15

3.1 The Jacobi Coordinates 18

3.2 Young Diagrams 35

3.3 Multi-trial SVM applied to ps^- 39

4.1 Convergence of SVM, Three Equal Mass Fermions 43

4.2 SVM and Sampling Distance Range 44

4.3 Two- and Three-Body Ground State Energy and Screening Length 45

4.4 Ground State Energy and Screening Length for $N = 3$ and 4 . 46

Chapter 1

Introduction

There are astonishing disparities between what we predict and what we see in many astrophysical phenomena. The galactic collision of Figure 1.1 is one of the most accessible observations of such a disparity. One can imagine how the collision played out: the two oblate galactic clusters careen toward each other and collide. Unsurprisingly, the luminous parts of both clusters interact and demonstrate clear collision features. However, most surprisingly, the mass centers of the two clusters pass through each other apparently unperturbed. Therefore we derive an important takeaway from Figure 1.1 for what will be discussed: whatever is making up the majority of the mass of those galaxies is interacting very weakly. The fact that the majority of mass is non-luminous is not unique to these galaxies.

Spiral galaxies have this mysterious non-luminous mass as well. They also provide understanding as to the structure of the mass, specifically in

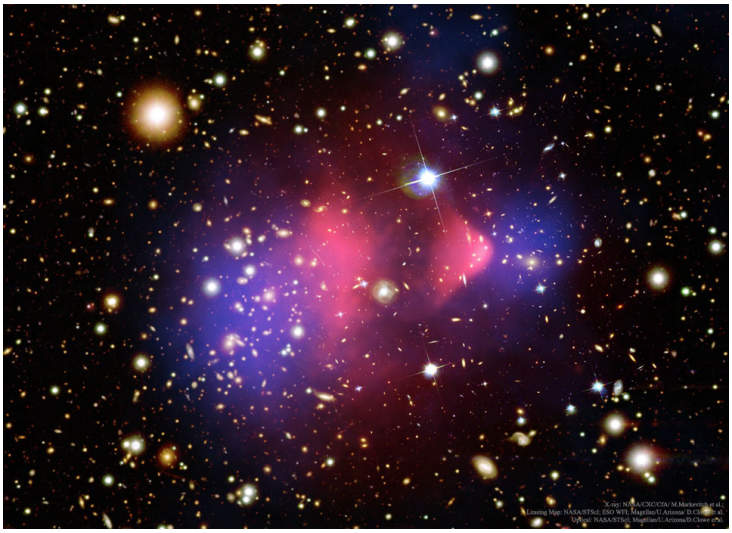

Figure 1.1: The Bullet Cluster, two galactic clusters post collision. The mass density is highlighted in blue and the light emitting region is highlighted in red [3].

the disparity found between theory and measurements of galactic rotation velocity as a function of the radius from the galactic center. Following the exposition given in [2], we first note that Newtonian mechanics implies that

$$v_c(r) = \sqrt{\frac{GM}{r}}, \tag{1.1}$$

where $v_c(r)$ is the circular velocity of the stars a distance r from a spiral galaxy's core, G is the gravitational constant, and M is the mass enclosed by r. Thus, if the mass was attributed only to luminous sources, once r is past the luminous disk of the galaxy, M would be constant, and $v_c(r) \propto 1/\sqrt{r}$. However, the rotation curves presented by Vera Rubin et. al. in 1980, depicted in Figure 1.2, contradict this expectation. The velocity curves

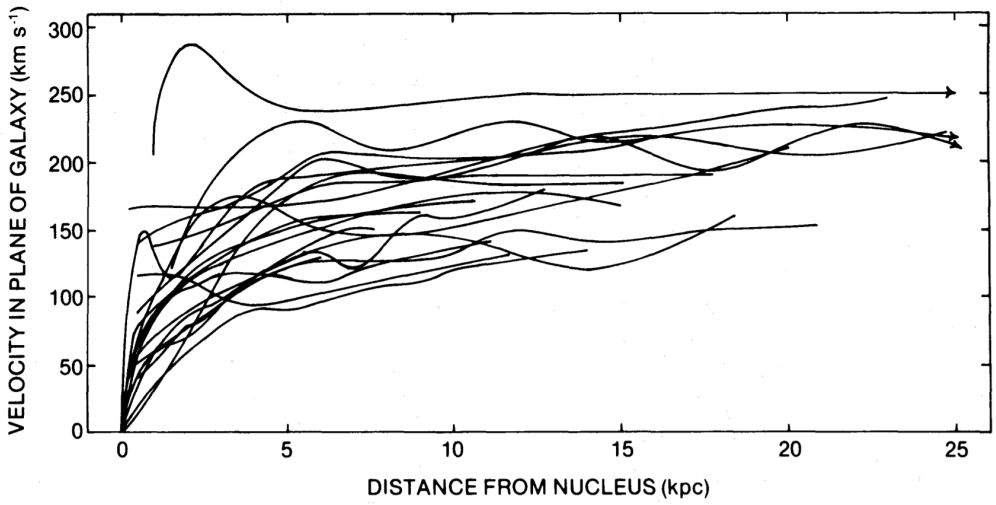

Figure 1.2: Original galactic rotation curves from Rubin et. al in 1980 [4]. Note that most curves flatten out at large distances.

flatten out at such distances. If we assume that our model of Newtonian gravity correctly approximates the rotation curve, then this implies that $M(r) \propto r$ past the luminous disc. There is invisible mass!

Is such invisible mass necessary? In the case of the galactic rotation curves, perhaps our model of gravity is incorrect. Many theories have gone this route—modifying the established theory of gravity—and fall into the class of Modified Newtonian Dynamics (MOND). They posit that the model of Newtonian gravity breaks down at small accelerations. Although rooted in an exciting premise and able to account for the dynamics of rotating galaxies, these theories have yet to be able to explain phenomena involving strong gravitational lensing, which fall in the regime of Newtonian gravity [5].

Furthermore, general relativity (which takes the form of Newtonian grav-

ity on these scales), is incredibly well tested. Most recently, the Advanced LIGO team announced detections of gravitational waves predicted by this theory, verifying it to a high degree. Interestingly, these detections have also ruled out many MOND theories [6], although some remain, making such a theory a possible and/or partial explanation.

Dark matter (DM) emerges when you assume the other direction: our theories of gravity are correct, or correct enough to not be able to explain such a discrepancy by themselves. To fully explain the flattening of the galactic rotation curves, there must be a halo of dark matter particles outside the luminous disk of the galaxy—particles that do not interact with light. Dark matter is hypothesized to make up the majority of the mass density of the Bullet Cluster. As indicated by the Bullet Cluster, these particles interact weakly with other particles and themselves, if at all.

1.1 Asymmetric Dark Matter

The amount of dark matter in the universe is greater than the amount of visible (baryonic) matter, matter made from neutrons and protons. In 2015, surveys of the Cosmic Microwave Background by the PLANCK collaboration indicated that dark matter makes up roughly 85% of the matter in the universe [7]. While this may seem like a vast difference, it is actually quite remarkable that the ratio of dark matter to visible matter is so close to one. At first glance, there is no reason why the ratio shouldn't be another much

larger or much smaller value.

This suggests that dark matter and visible matter perhaps originate together from some shared mechanism. We know that the current distribution of visible matter is a product of an asymmetry in the amounts of visible matter and antimatter in the early universe. After all the antimatter annihilated with matter, the universe was left with the matter that, over time, took on the present-day distribution.

Theories of Asymmetric Dark Matter (ADM) are motivated by these connections. They postulate that the evolution of the distribution of dark matter mirrors that of the distribution of visible matter: it is due to an asymmetry between dark matter and its antiparticle that originated in the early universe. Furthermore, they claim that these asymmetries are due to shared processes. The shared processes that generated matter/antimatter and dark matter/dark anti-matter ended in the early universe, the particles annhilated with their antiparticles and left the current distributions that are significantly similar.

One does not have to give significance to the similarity between DM mass density and baryonic mass density. The standard Weakly Interacting Massive Particle (WIMP) model for dark matter takes it to be a coincidence. This theory attributes the present-day dark matter distribution to the "freeze out" density, which corresponds to when the universe started expanding faster than would allow dark matter annihilation [8]. The "weakly interacting" part of the theory allows for dark matter to interact and annihilate into

non-DM particles.

Theories with DM asymmetry have propagated into distinct forms. Constraints established by many years of experiment have refined or extinguished many models that contain this feature. The asymmetric nature of DM is just one feature of ADM theories, and ADM currently stands outside of experimental constraint. This is one reason why significant development of the theory has occurred [9].

1.2 Overview

Theories of ADM predict an interaction between dark matter particles. If this interaction is attractive and strong enough, the dark matter particles can form bound states similar to atomic nuclei. Also like atomic nuclei, it is possible that certain numbers of dark matter particles are unstable as a single bound state, and would therefore decay into multiple smaller states. Such decay modes at certain particle numbers would significantly impact the present-day distribution of dark matter nuclei, both in terms of number and size.

We see this in the nucleosynthesis of normal elements during the early universe. It is known that there are no stable nuclei of 5 or 8 nucleons. This decay mode indicates a bottleneck in nucleosynthesis: atoms with numbers of protons and neutrons greater than that of the bottleneck would have to be formed while avoiding a configuration of 5 or 8 nucleons. This restricts

the paths possible in nucleosynthesis (hence "bottleneck") and elements past the bottleneck are therefore less ubiquitous.

By examining the ground state energy of the configurations of particles, one can determine whether or not such decay modes exist. For example, if the ground state energy of a three-body state is greater than that of a two-body state, we know that a three-body state would decay into the two-body state and a free particle, as it is energetically preferable.

The purpose of this analysis is to map the ground state energy of dark matter for few particles and determine whether decay modes—and therefore bottlenecks in dark matter nucleosynthesis—exist. Certainly, this map depends on the characteristics of the interaction between the dark matter particles, such as the range and strength.

We formalize these characteristics in Chapter 2, in which the two-body system is discussed. This chapter lends motivation and understanding that is utilized in the few-body case. Chapter 3 divulges the methods used and relevant knowledge needed to understand the few-body case. It also applies this knowledge to an example and calculates the ground state energy of positronium minus, two electrons and a positron.

Chapter 4 relays the original results about the few-body bound states and determines whether bottlenecks exist based on assumptions that are made about the interaction between the dark matter. Finally, Chapter 5 concludes in summary, with possible future research directions. Both the two-body and few-body calculations are implemented in *Mathematica 11.3* and

may be accessed at `https://github.com/AlexanderShaw/dm-calcs`. The notebooks contain additional technical details that expedite and optimize solutions.

Chapter 2

The Two-Body Problem

This chapter discusses the two-body bound state. It begins with a quick review of how we use Schrödinger's equation to model two particles interacting via pairwise forces. It then motivates the form of the interaction considered between dark matter particles. It concludes with results on the two-body bound state as this interaction changes, and indicates how these results guide the few-body problem.

2.1 Determining the Two-Body Ground State

Any good classical mechanics text discusses the system of two bodies, masses m_1 and m_2, interacting via some potential $V(r)$, where $r = |\vec{r}_1 - \vec{r}_2|$. We review the procedure that should be familiar: by introducing the center of mass (CM) coordinate $\vec{R} = (m_1\vec{r}_1 + m_2\vec{r}_2)/(m_1 + m_2)$ and relative coordinate

$\vec{r} = \vec{r}_1 - \vec{r}_2$ and enforcing conservation of angular momentum, one reduces the problem to that of describing a single body of reduced mass μ in the spherically symmetric potential $V(r)$ in the CM frame.

The same procedure may be applied in the quantum case.[1] Ultimately, one solves Schrödinger's equation through separation of variables, creating two uncoupled equations: one for the angular wavefunction, the other for the radial wavefunction. We call the radial wavefunction $\psi(r)$. The equation is:

$$\left(\frac{1}{r^2}\frac{d}{dr}r^2\frac{d}{dr} - \frac{l(l+1)}{r^2} + \frac{2\mu}{\hbar^2}[E - V(r)]\right)\psi(r) = 0. \tag{2.1}$$

In the ground state, we are concerned only with the case $l = 0$. In solving, it is useful to make the substitution $u(r) = r\psi(r)$, so the Dirichlet boundary conditions are zero, i.e. $u(0) = 0$ and $u(r) \to 0$ as $r \to \infty$. In this form, we get the equation

$$V(r)u(r) - \frac{\hbar^2}{2\mu}\frac{d^2u(r)}{dr^2} = Eu(r). \tag{2.2}$$

For an arbitrary potential, such a differential eigenvalue problem is difficult or impossible to solve analytically. However, this equation is simple to solve numerically using modern computational software. Given a potential, we numerically determine the entire eigensystem, which includes the ground state wavefunction and energy.

From here on, we use atomic units. By definition, this means that the

[1] See, for example, Chapter 5 in [10].

electron's mass m_e, the electron's charge e, Coulomb's constant k_e and $\hbar$ are set to 1. Since the fine structure constant is $\alpha = k_e e^2/\hbar c \approx 1/137$, we have that the speed of light is $c = 1/\alpha \approx 137$. Units of length are returned in terms of $a_0 = \hbar/(m_e c\alpha) = 1$, the bohr radius. Energies are returned in terms of hartree, but denoted by a.u. (atomic unit). One a.u. is $\alpha^2 m_e c^2 \approx 27$ eV.

Since we are concerned only with the ratio of the two-body ground state energy to the three- and four-body ground state energies, we assume henceforth that all dark matter particles have mass $m_e = 1$, implying that $\mu = 1/2$.

2.2 Yukawa Potential

This section motivates the form that $V(r)$ is assumed to take between dark matter particles. Recalling from Figure 1.1, we expect that dark matter interactions be weak and short ranged.

The particle theory of electromagnetic interactions is fundamental in particle physics theory. This theory models such interactions as the exchange of photons between charged particles.[2] In particle physics, interactions between particles are mediated by other particles.

In 1935, Japanese physicist Hideki Yukawa predicted that the short-range attractive interactions between protons and neutrons in nuclei are mediated by massive spin-0 particles called mesons [12]. Taking a hint from Yukawa, we assume that interactions between dark matter particles are mediated by

[2] An accessible text on this subject is [11]

some massive spin-0 particle of mass m_s.

From this, one can employ the tools of nonrelativistic quantum field theory and determine the potential $V(r)$ that results from such an interaction.[3] Here, we just cite the form that results from assuming a *scalar*—meaning spin-0—massive mediator:

$$V(r) = -\frac{\alpha_s}{r} e^{-r/\delta_s}, \tag{2.3}$$

where $\delta_s = \hbar/(m_s c)$ and c is the speed of light. Note the overall minus sign that implies this interaction is attractive.[4] The free parameters are α_s and δ_s. The parameter δ_s determines the range of the force, while α_s determines the strength.

Since we are concerned with the structure of solutions using these potentials, we ignore the overall strength and set $\alpha_s = 1$ (the strength of the Coulomb potential). Figure 2.1 depicts the form of this potential, which is called the *Yukawa potential*. In this figure, starting from $\delta_s \to \infty$, we get the Coulomb potential. As we decrease δ_s, the exponential shortens the range of the potential to the scale of δ_s. Naturally, the parameter δ_s is called the *screening length*, the length over which the potential is "screened" (reduced) by the exponential.

Classically, all the potentials in Figure 2.1 allow bound states. The quan-

[3] See [13], Chapter 1, for a physical and approachable derivation of the potential.

[4] Intuitively, as the mass of the mediator tends to 0, we get that $V(r) \to -\alpha_s/r$, which is the form of the familiar Coulomb potential. This is what we expect for an interaction mediated by a massless particle, i.e. the electromagnetic interaction!

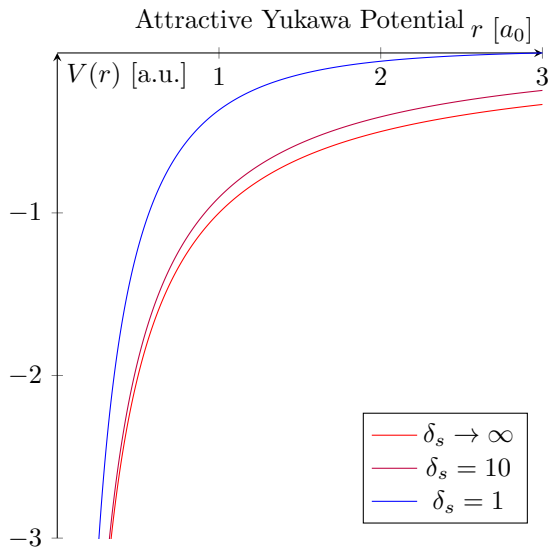

Figure 2.1: The attractive Yukawa potential with different screening lengths δ_s (a_0).

tum case is more complicated and we will find that this trend is not replicated. The following section details the structure of the solutions to Equation 2.2 as we vary over the free parameter δ_s.

2.3 Two Body Results and Discussion

The results of this section serve as reference for the few-body results. Two-body systems have many interesting features, but we focus only on the ground state energies and the general structure of the radial ground state wave-functions that solve Equation 2.2. We return to discussing these results in comparison to the few-body results in Chapter 4.

The attractive Yukawa potential becomes the Coulomb potential in the

limit $\delta_s \to \infty$. Introductory quantum mechanics courses usually spend extended time discussing the radial solutions for the Coulomb potential, for this is a fundamental part of the beautiful picture of hydrogen that quantum mechanics allows. It is well known that hydrogen has an infinite number of bound states, the basic structure having energies inversely proportional to the square of the principle quantum number; the energies are familiarly $E_n = -13.6 \text{ eV}/n^2$.

Due to the exponential screening term, the Yukawa potential allows only a finite number of bound states. As the screening length δ_s decreases, so too does the number of bound states. The value of δ_s corresponding to when the ground state energy is zero, i.e. when there are no bound states, is called the *critical* screening length. Figure 2.2a depicts our results in how the ground state energy changes with δ_s, and returns a critical screening length of $\delta_s^\circ = 1.68\ a_0$. The usual value reported for this is $0.84\ a_0$, but it is important to remember that we are considering identical particles of mass m_e, and thus the reduced mass is $\mu = 1/2$. When this is reported, it is usually with regards to a hydrogen-like system in which $\mu = 1$. This difference results in a factor of two on the critical screening length.

In the limit $\delta_s \to \infty$, calculation shows that the ground state energy converges to -0.25 a.u. $= -13.6/2$ eV, which is half the ground state energy of a system of particles with reduced mass the mass of the electron. This is the ground state energy of positronium (an electron and a positron). This agrees with what we know about hydrogen: Rydberg's Formula tells us that,

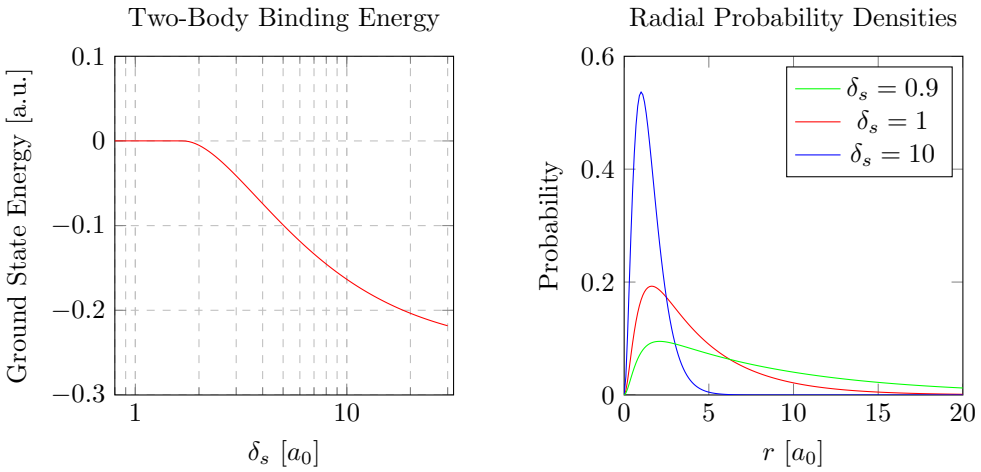

(a) The ground state energy with varying screening lengths. The critical screening length is calculated as $\delta_s^\circ = 1.68\ a_0$.

(b) The ground state radial probability distribution for different screening lengths.

Figure 2.2: The ground state energy and radial probability distributions for two particles interacting via an attractive Yukawa potential.

for the Coulomb potential, the ground state energy is proportional to the reduced mass.

We derive a significant takeaway for the following chapters from Figure 2.2b: the scale of the wavefunctions' spatial extent. As the screening length increases, the system becomes more tightly bound. Approaching the critical screening length, the ground state wavefunction becomes much larger in its spatial extent. As indicated in the figure, this effect is obvious when the screening length is very close to its critical value. In solving the few-body problem, we will need to specify the expected range that the spatial wavefunction occupies. From Figure 2.2b, we determine this to be approximately $0 - 10\ a_0$ and note that this only breaks down when very close to the critical

screening parameters.

We now have all we need from the two-body problem. We discuss the few-body problem in the next chapter.

Chapter 3

The Few-Body Problem

In this chapter, we work to understand how to generalize from the two-body case to N bodies. The initial step to 3 bodies builds up the concepts needed to understand N bodies. We then outline solution methods to the quantum 3-body problem, pick one (the *Stochastic Variational Method*), and analyze its performance on the known system ps^- (positronium minus), two electrons and a positron. Along the way, we discuss the relevant theory needed to understand the application of this method.

3.1 Introduction to the Quantum Few-Body Problem

We have discussed the solution of the two-body problem when we have a pairwise radial potential. Following that solution and borrowing from [14],

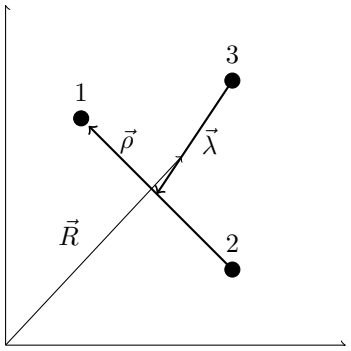

Figure 3.1: The Jacobi coordinates used in the three-body problem with equal mass particles, unscaled.

we now show exactly where the few-body problem initially becomes much more difficult. Consider the three-body Hamiltonian,

$$\hat{H} = \left(-\frac{\hbar^2}{2m_1}\nabla_1^2 - \frac{\hbar^2}{2m_2}\nabla_2^2 - \frac{\hbar^2}{2m_3}\nabla_3^2 + V(\vec{r_1}, \vec{r_2}, \vec{r_3}) \right) \tag{3.1}$$

In the two-body case, we introduced new coordinates that allowed us to use separation of variables to solve Schrödinger's equation easily with numerical methods. We can try and do the same thing in the three-body case. To simplify the discussion, let all particles be of equal mass m. Let,

$$\vec{R} = \frac{1}{\sqrt{3}}(\vec{r_1} + \vec{r_2} + \vec{r_3}),\ \vec{\rho} = \frac{1}{\sqrt{2}}(\vec{r_1} - \vec{r_2}),\ \text{and}\ \vec{\lambda} = \frac{1}{\sqrt{6}}(\vec{r_1} + \vec{r_2} - 2\vec{r_3}). \tag{3.2}$$

These coordinates are called *Jacobi coordinates*, and they are depicted in Figure 3.1. The vector $\vec{R}$ is the center of mass vector, the vector $\vec{\rho}$ is the vector from particle 1 to particle 2 and $\vec{\lambda}$ is the vector from particle 3 to the center of mass of particles 1 and 2. By renaming the particles, there are three

equivalent representations of the orientation of particles 1, 2 and 3 about the center of mass with different $\vec{\rho}$ and $\vec{\lambda}$. Note that the coordinates are scaled such that (as one can show through direct substitution of variables):

$$\nabla^2_{\vec{R}} + \nabla^2_{\vec{\rho}} + \nabla^2_{\vec{\lambda}} = \nabla^2_{\vec{r_1}} + \nabla^2_{\vec{r_2}} + \nabla^2_{\vec{r_3}}. \tag{3.3}$$

Due to the equal mass condition, there are no cross terms. These cross terms do not prohibit an easier solution, but they would complicate the discussion. Consider now the equation we are trying to solve:

$$\frac{\hbar^2}{2m}\left(-\nabla^2_{\vec{R}} - \nabla^2_{\vec{\rho}} - \nabla^2_{\vec{\lambda}} + V(\vec{R},\vec{\rho},\vec{\lambda})\right)\Psi(\vec{R},\vec{\rho},\vec{\lambda}) = E\Psi(\vec{R},\vec{\rho},\vec{\lambda}) \tag{3.4}$$

If the potential is the sum of parts, each depending only on one of $\vec{R}$, $\vec{\rho}$ or $\vec{\lambda}$, then we may use separation of variables to produce three uncoupled equations in each of these three coordinates, which are easily solved.

As demonstrated in [14], the only potential that allows this is one in the form of a harmonic oscillator. Generally, the potential is not be the sum of independent parts, and we are unable to separate into uncoupled equations. We must then seek solutions with other approximate methods.

These methods can take many forms and each has its strengths and weaknesses. For our purposes, we seek a method that is easily generalizable to larger numbers of identical particles. What follows is an overview of the different methods of solution of few-body systems and justification for the method selected in this analysis.

3.2 Methods of Solving the Quantum Few-Body Problem

The optimal method of solution depends greatly on the problem being solved. To reiterate, we want a method of solving the ground state energy of a system of identical particles. According to [1], the Faddeev method gives the most precise answers to the three-body problem.

This method involves separating the wavefunction into three components, each representing the three-body system by one of the equivalent coordinate sets of Figure 3.1. This representation allows one to turn the Schrödinger equation into a set of coupled differential equations that are numerically solvable. Although this method is very precise, it is very difficult to generalize to four particles and beyond. The reader is directed to [15] for an extensive discussion of the Faddeev method.

Another method is the hyperspherical harmonics expansion method. This method expands the wavefunction in a way analogous to how one expands the two-body angular wavefunction in terms of spherical harmonics. It does this by mapping the function onto a hypersphere, using a hyperradius and a set of angles as coordinates. It then seeks to solve the Schrödiger equation when the infinite expansion in terms of the hyperspherical harmonics is truncated at some finite number of terms. As discussed in [1], determining the correct symmetrization to use in the expansion when dealing with identical particles is a difficult problem and limits the method to up to 5 bodies. This difficulty

and limit makes it an undesirable method for our purposes. This method is discussed in-depth in [16].

These two methods are some of the most popular in solving quantum mechanical few-body problems. Although they fall out of the general scope of our problem, they could be used as verification for the method we choose to pursue. There are multiple methods that allow a solution for more identical particles. The most accessible of them is the Stochastic Variational Method (SVM) discussed in [1], which we choose to apply to our problem. It will be demonstrated to be quite powerful in determining ground state energies.

3.3 Introduction to the Stochastic Variational Method

The SVM gives an upper bound on the ground state energy of a system of N particles and an approximate wavefunction for each energy level. In this work, we focus only on the ground state energy. The method is the subject of Suzuki and Varga's title, *Stochastic Variational Approach to Quantum-Mechanical Few-Body Problems*, and the following discussion draws extensively from this book.

A key part of the SVM is that it is *variational*, meaning that it relies on the quantum-mechanical variational method. This variational method takes

the form of the following identity:

$$E_0 \leq \frac{\langle \Psi | \hat{H} | \Psi \rangle}{\langle \Psi | \Psi \rangle}, \tag{3.5}$$

where E_0 is the ground state energy of the Hamiltonian $\hat{H}$, and $|\Psi\rangle$ is any wavefunction in the correct subspace of the Hilbert space of $\hat{H}$.[1] This result is actually quite intuitive when the spectra of $\hat{H}$ is discrete, which is the case we are concerned with. Since $\hat{H}$ is hermitian, we know that its eigenstates are orthonormal and span the whole space. That is, in the discrete case with $\{|\psi_i\rangle\}$ representing the set of eigenstates, we have:

$$|\Psi\rangle = \sum_i c_i |\psi_i\rangle , \tag{3.6}$$

for some $\{c_i\}$. We see that if $\{E_i\}$ is the set of energy eigenvalues, then

$$\langle \Psi | \hat{H} | \Psi \rangle = \sum_{i,j} c_i^* c_j E_j \langle \psi_i | \psi_j \rangle = \sum_i |c_i|^2 E_i \geq E_0 \sum_i |c_i|^2 = E_0 \langle \Psi | \Psi \rangle . \tag{3.7}$$

The inequality follows in that $E_0 \leq E_i$ for all i, implying Equation 3.5.

This upper bound varies as $|\Psi\rangle$ changes, and approaches the actual value E_0 as $|\Psi\rangle \rightarrow |\psi_0\rangle$. Optimization of $|\Psi\rangle$ in the full Hilbert space is too complicated, but we may restrict ourselves to a finite dimensional subspace of the Hilbert space by an expansion on this principle called the *Ritz Variational*

[1] This latter restriction is important in understanding how this method could distinguish between the subspace occupied by bosons and that of fermions, which is discussed later in Section 3.6.

Method, discussed in Appendix A.

The essence of this extension is the following: we may use any set of independent basis states $\{|\psi_i\rangle\}$ in the subspace defined by the problem, calculate a Hamiltonian matrix H and an overlap matrix B defined by

$$H_{ij} = \langle\psi_i| \hat{H} |\psi_j\rangle \qquad \text{and} \qquad B_{ij} = \langle\psi_i|\psi_j\rangle \,, \tag{3.8}$$

solve the generalized eigenvalue problem

$$H\vec{v} = \epsilon B\vec{v}, \tag{3.9}$$

and take the minimum such ϵ as an upper bound on E_0.

The basis functions $\{|\psi_i\rangle\}$ are chosen as to minimize the upper bound derived from this method.

There is a mathematical result that helps optimize the basis functions. Given a basis of size k with a corresponding upper bound ϵ_0, if we add any basis vector to the set and calculate the new upper bound ϵ_0', then we are guaranteed that $\epsilon_0' \leq \epsilon_0$.[2]

Although, in principle, we may immediately find an upper bound with a given basis set and minimize the upper bound with respect to the parameters the basis functions depend on, this is in practice less effective and more computationally demanding than the following natural alternative.

When increasing the basis size, we are guaranteed to lower the upper

[2]A proof of a more general result that implies this fact is given on p. 27 in [1].

bound. This fact allows the optimization of basis vectors one at a time: given a set of candidate vectors, we may choose the optimal vector to add to the basis by determining which candidate minimizes ϵ_0'. We then only have to generate a small basis set with a manageable number of parameters to start this process.

An algorithm is now clear that may converge on an accurate upper bound:

1. Choose a basis set to start from and calculate ϵ_0.
2. Generate a set of candidate vectors and for each candidate calculate ϵ_0', the upper bound corresponding to the basis including a candidate vector.
3. Append the candidate vector with minimum ϵ_0' to the basis and repeat steps 2 and 3 until convergence.

The upper bound converges to the exact ground state energy as long as the basis vectors chosen from span the entire space defined by the Hamiltonian.

3.4 Basis Vectors and Matrix Elements

The SVM uses correlated gaussians as its basis vectors, the general form of which are

$$\psi = e^{-\frac{1}{2}\sum_{j>i=1}^{N}\alpha_{ij}(\vec{r}_i-\vec{r}_j)^2}, \tag{3.10}$$

where $\vec{r}_i$ is the position vector of the ith particle. Since $(\vec{r}_i-\vec{r}_j)^2$ is the square of the distance between particle i and j, we see that α_{ij} characterizes how

fast the wavefunction falls off as distance between particles i and j increases. Therefore, we see that $1/\sqrt{\alpha_{ij}}$ is the expected distance particles i and j are from each other. Combining this interpretation with the two-body results will guide the generation of the parameters $\{\alpha_{ij}\}$.

One main benefit of these basis functions is that the matrix elements of H and B are analytically calculable with the pairwise potentials we use. When optimizing a basis vector to produce the lowest upper bound, having analytical formulas for the matrix elements makes the calculations manageable, which is necessary because computational time and power will be a limiting factor.

The second advantage is that the basis vectors are *complete*. This means that the set of all correlated gaussians spans the Hilbert space. This implies that a systematic increase in basis size, like in the algorithm described, converges on an exact eigenvalue in the limit of large basis sizes; we are guaranteed that our algorithm will eventually converge to the actual ground state energy.

Switching to a relative coordinate system greatly simplifies the generation of the basis vectors and the calculation of the matrix elements. The Jacobi coordinates of Figure 3.1 can be generalized to N particles. For a system of N particles, let us denote by $\mathbf{r}$ the vector of vectors $\vec{r}_i$. Bold-faced vectors will denote vectors of vectors, while vectors denoted with arrows are tuples of real numbers. In switching to the generalized Jacobi coordinates, we set our frame as the CM frame and characterize the wavefunction by $N-1$ coordinates.

If we label the N particles from 1 to N, then the relative coordinates $\vec{x}_i$ are made according to the recursion:

$$\vec{x}_i = (CM \text{ of particles 1 to } i) - \vec{r}_{i+1}. \tag{3.11}$$

So, we have that, in the case of three equal mass particles: $\vec{x}_1 = \vec{r}_1 - \vec{r}_2$ and $\vec{x}_2 = (\vec{r}_1 + \vec{r}_2)/2 - \vec{r}_3$: this recursion generates the Jacobi coordinates in the three-body case. Let $\mathbf{x}$ denote the vector of $\vec{x}_i$. As more rigorously discussed in [1], since $\mathbf{x}$ characterizes the configuration of the N particles, we can find an $(N-1) \times 1$ coefficient vector $\vec{w}_{ij}$ such that

$$\vec{r}_i - \vec{r}_j = \vec{w}_{ij} \cdot \mathbf{x} = \vec{w}_{ij}^T \mathbf{x}. \tag{3.12}$$

In the aim of simplifying Equation 3.10 in terms of relative coordinates, consider that

$$\sum_{j>i=1}^{N} \alpha_{ij} (\vec{r}_i - \vec{r}_j)^2 = \sum_{j>i=1}^{N} \alpha_{ij} (\vec{w}_{ij} \cdot \mathbf{x})^2 \tag{3.13}$$

$$= \sum_{j>i=1}^{N} \alpha_{ij} (\mathbf{x}^T \vec{w}_{ij})(\vec{w}_{ij}^T \mathbf{x}) \tag{3.14}$$

$$= \mathbf{x}^T \left(\sum_{j>i=1}^{N} \alpha_{ij} \vec{w}_{ij} \vec{w}_{ij}^T \right) \mathbf{x}. \tag{3.15}$$

If we define A such that

$$A_{kl} = \sum_{j>i=1}^{N} \alpha_{ij} (\vec{w}_{ij} \vec{w}_{ij}^T)_{kl}, \tag{3.16}$$

then we have that

$$\psi = e^{-\frac{1}{2} \sum_{j>i=1}^{N} \alpha_{ij} (\vec{r}_i - \vec{r}_j)^2} = e^{-\frac{1}{2} \mathbf{x}^T A \mathbf{x}}. \tag{3.17}$$

We have now reparameterized the wavefunction in terms of the $(N-1) \times (N-1)$ symmetric matrix A. One can show that ψ is normalizable if and only if A is positive-definite. This property is necessary to enforce when generating these basis vectors.

The formulas for the matrix elements of H and B given ψ, as to be used in this analysis, are found in [1].[3]

It is crucial to remember that the total wavefunction Ψ be *in* the subspace defined by our problem and $\hat{H}$. This requires us to ensure that Ψ has the correct symmetrization that our problem calls for.

The following section discusses why we have this symmetrization requirement and how it is correctly enforced.

[3]Specifically, on p. 124 with definitions of terms found earlier in the text.

3.5 Indistinguishable Particles

Everyday life enforces the notion that, given any collection of identical objects, the objects are distinguishable if we are allowed maximum information about the system. For example, say a master juggler is about to juggle three identical tennis balls. Before the juggler starts, an intent observer may identify and label the tennis balls by their order in space. During the juggling, then, the observer may still distinguish the balls based on their tracking of the balls' movements.

If the juggler is good enough, it is likely that the observer will lose track of which ball is which, and thus the balls become somewhat, or fully, indistinguishable to them relative to their initial ordering. However, this indistinguishability is a result of a loss of information. Somewhere along the line, the observer lost track of the path of one or more of the balls. This reflects a classical lack of knowledge; if the observer had been tracking the balls' positions close enough, they could have *in principle* distinguished the tennis balls no matter their paths taken.

The above discussion regards loss of information relative to the initial ordering. Given a classical arrangement of objects, each will have a definite position and therefore each object is distinguishable from the rest by simply labeling it by its unique coordinates (certainly no two objects could occupy the same exact coordinates, classically). Usually though, we are interested in distinguishing objects as they evolve in time from previous states, rather

than at an isolated instant.

The uncertainty principle tells us that the question of the exact position of a quantum particle is undefined. Sure, if we separate two electrons enough in space, we may label one roughly as "here" and the other as "over there", but if we bring them close enough such that their wavefunctions overlap, who can say which is which? We know that the notion of a precise path must be undefined for such particles, so if a collection of them is juggled about close enough together, then it is impossible to distinguish them as they evolve in time.

Since the maximum amount of knowledge we are allowed about the orientation of the system is the wavefunction, even in principle we will not be able to distinguish the particles that will form the bound states we are concerned with!

If we have two particles, what does this fundamental indistinguishability imply about the wavefunction? Consider the operation of *permutation* of the particles. If we are to swap the position of the particles, we should be left with a completely indistinguishable wavefunction; any measurement we could perform on it would have the same expected results as the unpermuted wavefunction. Most generally, this implies that the operation will result in some global phase factor. Repeating the permutation operation again, we should get back the original wavefunction, with no global phase. This implies that the phase factor must be either ± 1.

This same argument above works when we consider pairwise permuta-

tions applied to a wavefunction of any number of identical particles. A wavefunction such that pairwise permutation results in a phase of $+1$ is called *symmetrical*, i.e. it is symmetric under permutation. A wavefunction such that pairwise permuation results in -1 is *antisymmetrical*. To illustrate, with two particles characterized by p_1 and p_2 and the permutation operator denoted by $\hat{P}$, then antisymmetry implies

$$\hat{P}\Psi(p_1, p_2) = \Psi(p_2, p_1) = -\Psi(p_1, p_2), \tag{3.18}$$

while symmetry implies that

$$\hat{P}\Psi(p_1, p_2) = \Psi(p_2, p_1) = \Psi(p_1, p_2). \tag{3.19}$$

The particles that obey these two symmetries require completely different statistical treatments when we want to answer questions about them. These are *Bose-Einstein statistics* for symmetric particles and *Fermi-Dirac statistics* for antisymmetric particles. The *Spin-Statistics Theorem* tells us that fermions obey Fermi-Dirac statistics, while bosons obey Bose-Einstein statistics.

A very relevant implication of antisymmetrical wavefunctions is the *Pauli principle*, that states no two fermions may be in the same state at the same time. Bosons, on the other hand, may be.

Given a system of identical fermions interacting via an attractive force, strong enough to form bound states, we expect that the bound state has a

size larger than that resulting from bosons. If we have a system of identical bosons in the same scenario, then the particles can be in the same state. We expect that their wavefunctions overlap more (in order to minimize the potential energy) and that the size of the total wavefunction would be smaller. We therefore surmise that the total energy of the arrangements would be different, with the bosons occupying a lower total energy state.

The pressure that prevents fermions from being in the same state is called *degeneracy pressure*. An example of the consequences of this pressure is the neutron star. The neutron has spin 1/2 and therefore obeys the Pauli principle. A simple description of the neutron star is that it has compressed the neutrons to the point that gravity is in equilibrium with the degeneracy pressure. This pressure is what prevents most stars from collapsing in on themselves and forming black holes and is one reason neutron stars are incredibly interesting.

The following two sections are more technical and derive much of their content from [10]. Their subject matter skirts the field of mathematics called representation theory and the interested reader is encouraged to understand how the following fits in that field.

3.6 Exchange Interaction

It is now evident that we must specify what symmetry particles have before asking questions about them. However, consider the time independent

Schrödinger equation. If the potential is independent of spin, then the Hamiltonian contains nothing regarding the spin of the wavefunction. Denote the spins of the particles by σ and the positions by $\mathbf{r}$. In the typical method of separation of variables, we can then view a wavefunction $\Psi(\mathbf{r}, \sigma)$ as

$$\Psi(\mathbf{r}, \sigma) = \eta(\sigma)\phi(\mathbf{r}) \tag{3.20}$$

where η is the called the *spin wavefunction*, and ϕ is the *position wavefunction*.

The energies determined by the Schrödinger equation depend only on ϕ. By the previous discussion, we expect that bosons and fermions find ground states at different energies when they are interacting via the same potential. If the energies found through Schrödinger's equation do not depend on the spins of the particles, how then do we know if a solution corresponds to a fermion or a boson?

The answer lies in the fact that ϕ contains more information than just the positions of the particles. It also contains information about the symmetrization of the total wavefunction; we know that $\Psi = \eta\phi$ must be either symmetric or antisymmetric with respect to pairwise interchange of particles.

Solutions for ϕ and its respective energy that correspond to a symmetric Ψ describe bosons, and those that correspond to antisymmetric Ψ describe fermions. This association is called the *exchange interaction*.

In general, there are many types of symmetries for η and ϕ that allow

either a symmetric or antisymmetric product. A symmetry of a wavefunction can be defined in terms of what the permutation operators do to the wavefunction. In these terms, as an example of another symmetry, it is conceivable that a few-body position wavefunction be symmetric in some particles, but neither symmetric nor antisymmetric in others.

For the SVM, in order for the trial functions to give an upper bound on the ground state we are concerned with, they must have the requisite symmetry. This is achieved by multiplying by a symmetrization factor, which is a combination of permutation operators.

3.7 Symmetrization

This section will discuss how the symmetrization that is enforced on the basis functions is determined by the system we are considering.

Let $\Psi(p_1, p_2)$ be a two particle wavefunction, where p denotes the spin and position of the particle, and consider the following formulations using the permutation operator of $\hat{P}_{12}$ that interchanges the particles:

$$\Psi_A \equiv \frac{\Psi(p_1,p_2) - \hat{P}_{12}\Psi(p_1,p_2)}{\sqrt{2}} = \frac{\Psi(p_1,p_2) - \Psi(p_2,p_1)}{\sqrt{2}}, \tag{3.21}$$

$$\Psi_S \equiv \frac{\Psi(p_1,p_2) + \hat{P}_{12}\Psi(p_1,p_2)}{\sqrt{2}} = \frac{\Psi(p_1,p_2) + \Psi(p_2,p_1)}{\sqrt{2}}. \tag{3.22}$$

The wavefunction Ψ_A is antisymmetric with respect to interchange of particles, while Ψ_S is symmetric with respect to interchange of coordinates. Given

any $\Psi(p_1, p_2)$, we build a state with the requisite symmetry by these operations, which we denote by $\hat{A}$ and $\hat{S}$ respectively. The factor of $1/\sqrt{2}$ is included for normalization.

We generalize this procedure for a wavefunction describing a system of N particles, say $\Psi(p_1, \ldots, p_N)$. There are $N!$ possible permutations that can be made on this wavefunction. For a wavefunction Ψ_S that is symmetric with respect to every particle, we know that for an arbitrary permutation $\hat{P}$, we have $\hat{P}\Psi_S = \Psi_S$. For a completely antisymmetric Ψ_A, we would have that $\hat{P}\Psi_A = \text{par}(P)\Psi_A$. The parity of P is denoted $\text{par}(\hat{P})$, and it is -1 if the permutation is odd, while $+1$ if the permutation is even.[4]

The operation of antisymmetrization with respect to a given subset of particles $\{i, \ldots, k\}$ is denoted by $\hat{A}_{i\ldots k}$, and similarly $\hat{S}_{i\ldots k}$ for symmetrization. Denote by $\mathbb{X}$ the power set of $\{i, \ldots, k\}$. The general form of $\hat{A}_{i\ldots k}$ and $\hat{S}_{i\ldots k}$ can thus be seen as

$$\hat{A}_{i\ldots k} = C \sum_{a \in \mathbb{X}} \text{par}(\hat{P}_a)\hat{P}_a, \tag{3.23}$$

$$\hat{S}_{i\ldots k} = C \sum_{a \in \mathbb{X}} \hat{P}_a, \tag{3.24}$$

where C is a normalization constant. It is recommended that the reader convinces his or her self that $\hat{A}_{i\ldots k}\Psi(p_1, \ldots, p_N)$ has the expected symmetry, and similarly for $\hat{S}_{i\ldots k}\Psi(p_1, \ldots, p_N)$.

[4]Every permutation can be decomposed into a composition of multiple pairwise permutations. The parity of the number of pairwise permutations is a fixed characteristic of the permutation, and thus determines an *odd* or *even* permutation.

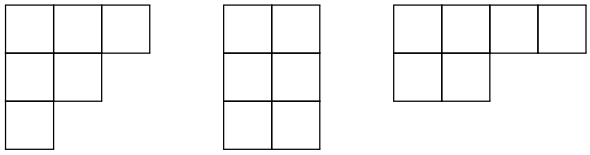

Figure 3.2: Young diagrams for 6 particles.

Using these two operations, we can generate all the possible types of symmetry of Ψ. However, we know Ψ must be entirely antisymmetric or symmetric with respect to interchanges of particles. Therefore we discuss how to symmetrize ϕ and η such that their product has the same expected symmetry as Ψ.

First, we consider the possible symmetries of ϕ. Symmetries corresponding to applications of $\hat{A}$ and $\hat{S}$ can be visualized by *Young diagrams*, examples of which are depicted in Figure 3.2.

A general Young diagram for an N particle system is an arrangement of N boxes in rows and columns, with the length of the rows decreasing down the diagram. There are the same number of Young diagrams for N boxes as there are partitions of N, that is, the number of solutions to $n_1+n_2+\ldots = N$, where each n_i is a positive integer.[5]

Using a Young diagram, a symmetry of ϕ is generated by the following procedure:

1. Label each cell of the diagram with a unique number 1 to N,

2. Symmetrize ϕ with respect to the variables in each row,

[5]A formula for this number as a function of N is unknown and an interesting problem in its own right!

3. Antisymmetrize ϕ with respect to the variables in each column.

All possible symmetries of ϕ are generated by this procedure applied to all possible Young diagrams. For example, the completely symmetric state is generated by a single row. One could perform the symmetrization steps in reverse, but they would produce a set of linearly dependent ϕ with respect to the procedure given above. Labelling without unique numbers will also produce linearly dependent symmetries, or zero (for example, antisymmetrizing with respect to variables that are already symmetrized will give zero).

Consider particles with integral spin. The total wavefunction must be completely symmetric. For this to be so, it must be that the symmetry of the position and spin functions are given by the same Young diagram [10].

If the particles have half-integral spin, then the Young diagram of the position function is the transpose of that of the spin function, in order for the total wavefunction to be antisymmetrical.

This immediately implies that, for a system of spin-1/2 particles, we may have at most two rows in a Young diagram describing the symmetry of the spin wavefunction. Since the particles' spin coordinates can only be up or down, if we had a column of 3 variables, then at least two variables in the column would be the same. Antisymmetrizing with respect to variables that are the same results in zero, so we conclude that a column with three variables is not allowed.

A similar argument implies that for spin-0 particles the spin state cannot be antisymmetrized at all, and thus the corresponding Young Diagram is a

single row for the positional wavefunction.

For spin-1/2 particles, it can be shown that if N is the difference between the lengths of rows in the Young diagram, then the corresponding total spin is $S = N/2$, recalling $\hbar = 1$.[6] This one-to-one correspondence with the Young diagrams and total spin holds only for systems of particles with spin 1/2.

As discussed in Section 3.6, a symmetry of ϕ corresponds to a set of energy levels. For spin-1/2 particles, the symmetry of ϕ is directly related to the total spin of the system through the symmetry of η.

In relation to the SVM, it is now clear how to determine the symmetry of the trial functions to solve the ground state for a collection of spin-1/2 particles (and for a collection of spin-0 particles). This symmetry is exactly the symmetry determined from the position Young diagram corresponding to the lowest possible total angular momentum.

3.8 Application to ps^-

We now have all the requisite understanding to apply the SVM to a system of spin-1/2 particles. Consider ps^-, two electrons and a positron. This system has a measured ground state energy of -0.262005 a.u. [1]. The particles will interact pair-wise via a $1/r$ potential, either repulsive or attractive depending on the pair considered. Label the positron as particle 1, and the electrons as particles 2 and 3.

[6] The reasoning behind this relation between the total spin of the system and the Young diagram is explained on p. 214 in [10].

The symmetrization requirement is enforced quite simply since we only have two indistinguishable particles (the two electrons). The total wavefunction must be antisymmetric with respect to interchange of particles 2 and 3. This is achieved through ϕ being completely symmetric and η being antisymmetric with respect to particles 2 and 3, or vice versa.

We need the total angular momentum to be the minimum allowable $\hbar/2$. This is achieved through either the two electrons having the same spin state, corresponding to antisymmetric η or through the two electrons having opposite spins, corresponding to symmetric η. We are guaranteed that the total spin of the system is $\hbar/2$ when the two electrons have opposing spins. Therefore, we choose η as antisymmetric, so the positional wavefunction ϕ must be completely symmetric.

Thus the total positional wavefunction will look like

$$\Phi(\mathbf{x}) = \sum_i c_i (1 + \hat{P}_{23}) e^{-\frac{1}{2}\mathbf{x}^T A_i \mathbf{x}}. \tag{3.25}$$

Recall that the coefficients $\{c_i\}$ are solved for in the generalized eigenvalue problem of the Ritz Variational Method.[7]

We implement the algorithm outlined in Section 3.3 to find an upper bound on the ground state energy of this system, using the given formulas for the matrix elements in [1] and abiding by a random generation of the $\{A_i\}$.

[7]See p. 15 in [1] for the form of $\hat{P}_{23}$ in terms of its action on A_i.

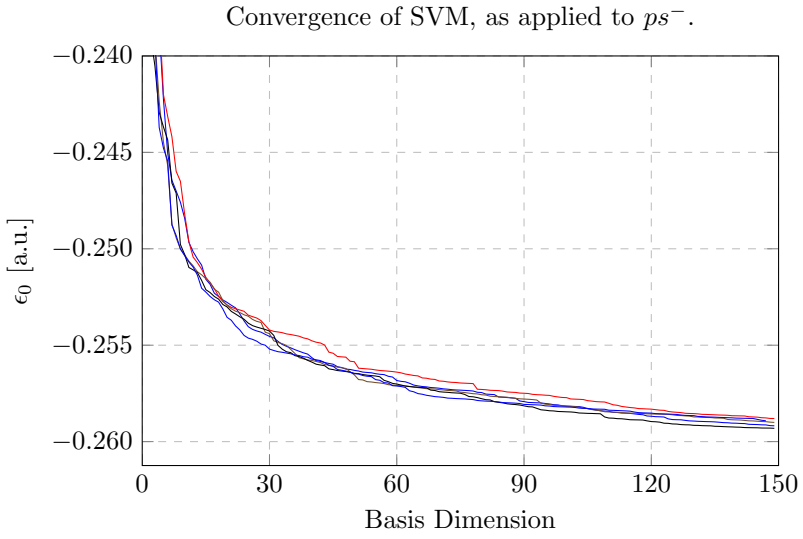

Figure 3.3: The SVM applied to ps^- over 5 trials.

This random generation is done via selecting the elements of A_i according to the intuition derived in Section 3.4, that the distance between particles i and j corresponds to $1/\sqrt{\alpha_{ij}}$. For the wavefunction to be normalizable, it is also necessary to enforce positive-definiteness. Based on the results of the two-body analysis, we know that the electron and positron would be roughly within 0 – 10 a_0 of each other, so we sample $1/\sqrt{\alpha_{12}}$ and $1/\sqrt{\alpha_{13}}$ in this range. It is expected that the two electrons are further from each other, so we select $1/\sqrt{\alpha_{23}}$ in the range of 0 – 20 a_0.

The upper bound returned by the SVM is denoted ϵ_0. The results of the SVM over multiple trials are given in Figure 3.3. As is depicted, the method converges toward the measured ground state energy of ps^- for every trial, always returning an upper bound within 1% of the measured -0.262005 a.u. As demonstrated in [1], one can extend the basis size to 600 and refine the basis

elements (such that they produce a lower energy) to the point of agreement up to 10 digits.

These results assure that it is possible to implement the SVM to very accurate ends. Unfortunately, time and computational resources prevent this analysis from reaching large basis sizes and implementing refinement. In this implementation of the SVM, doubling the basis size to 300 produces an upper bound of -0.259938 a.u.

An extended analysis of different basis vector selection procedures as applied to the ps^- system is given in [1].

As the method was applied to ps^-, it may be applied to systems of our interest.

Chapter 4

Results and Discussion

The Stochastic Variational Method was applied to systems of equal mass spin-1/2 particles. We assume that the particles interact pair-wise through a Yukawa potential, as those discussed in Chapter 2. Time and computational resources limited the analysis to 3 and 4 bodies.

Since the SVM gives an upper bound, we do not know when we have converged to the exact value of the ground state energy. Ideally, the method would be complemented by a lower bound. This is possible, although not implemented in this analysis.[1]

It may be that a lower bound is not necessary. It is expected that the wavefunctions of these systems are highly symmetric and therefore a good approximation can be made with gaussians. This would imply that the convergence should occur relatively quickly (compared to ps^-).

[1] See Section 3.2 p. 30 in [1] for a discussion on how to establish a lower bound.

Figure 4.1 shows multiple applications of the SVM to systems of three spin-1/2 particles for different screening lengths. The distances between particles are sampled from $0 - 10\ a_0$, following the results of the two-body problem (Section 2.3). As is demonstrated, they converge to a value quite quickly. Three trials for each potential are shown, and they each converge to the same value.

As it stands, it is unknown whether this value is of the exact ground state. It may be that the method converges to a non-physical limit. Since the gaussians are complete, this is only possible if the selection procedure is biased. If the exact ground state wavefunction is not within the span of the gaussians sampled from, such an artificial limit is anticipated.

It is expected that as the ground state energy of a bound system tends toward 0, the system becomes less bound and the particles become further apart on average. Decreasing the ground state energy would constrict the particles together. This intuition was verified in the two-body case. Therefore, in checking that the wavefunctions near the three-body critical screening length (which will be discussed) fall within the span of the gaussians sampled with distances $0 - 10\ a_0$ guarantees that the stronger-bound systems also do. Figure 4.2 demonstrates that as the sampling range is increased, the method still converges to the same value within a range of roughly 0.0025 a.u. This is tolerable for this application, so the sampling between $0 - 10\ a_0$ is considered to not produce an artificial limit.

We must decide a basis dimension to apply over the same δ_s range as in

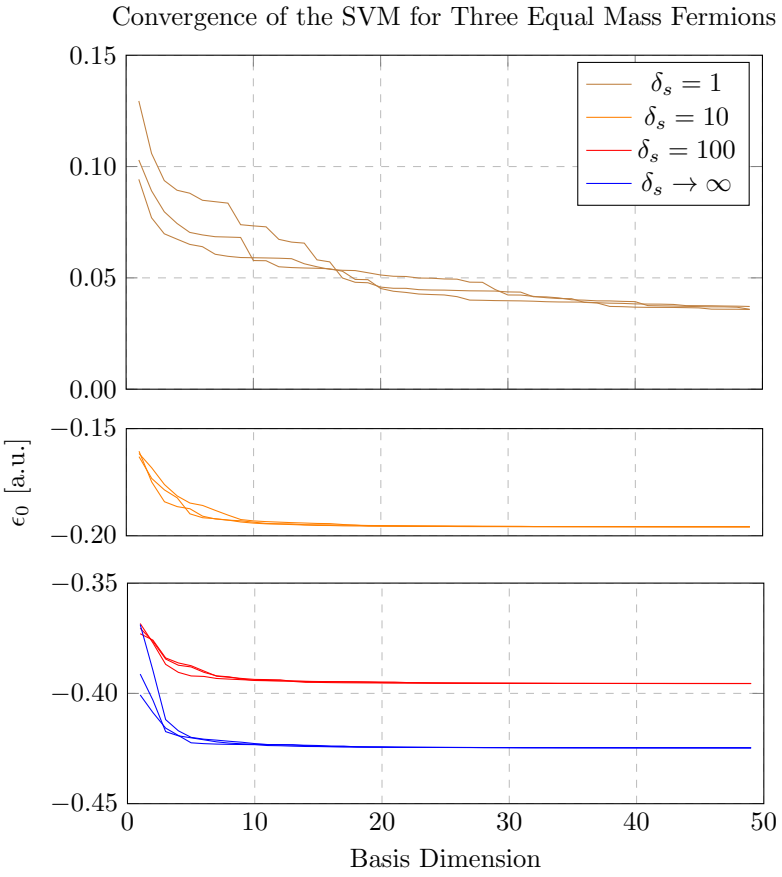

Figure 4.1: The SVM applied to three-body fermionic systems of equal mass particles, interacting via a pairwise attractive Yukawa potential of screening length δ_s (a_0). Interaction with hydrogen potential (blue) is also included.

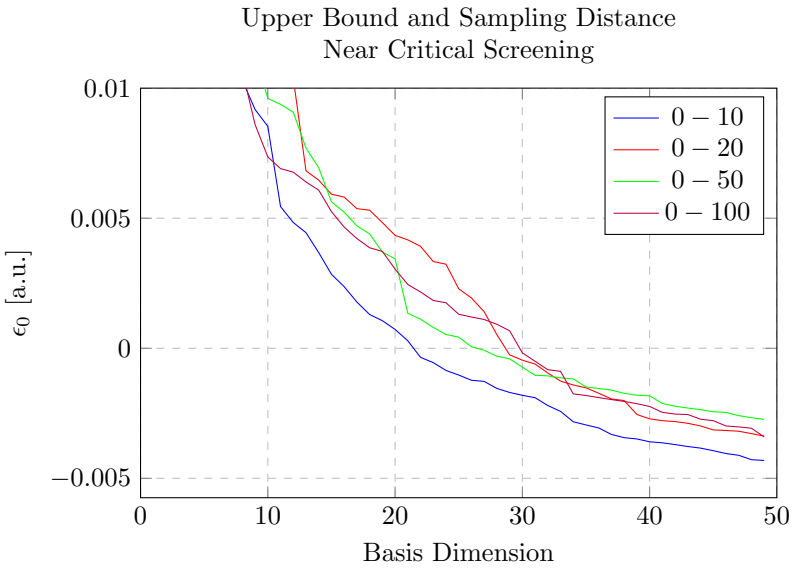

Figure 4.2: The SVM applied to a three-body fermionic system near the critical screening length, at $\delta_s = 3\ a_0$. Different distance ranges (a_0) are sampled from for each trial.

the two body case. This decision is largely based on available computational resources. This analysis uses a maximum basis size of 20 and based on Figure 4.1, it is reasonable that the actual ground state energy is within roughly 0.02 a.u. of the upper bound. We propagate this error in the figures and emphasize that this error is an estimate, for we have no formal lower bound on the ground state energy. It is motivated by the evidence that the method is converging to the actual ground state energy, and by the scale on which it is doing so.

The results of the three-body calculations are given in Figure 4.3. Using this figure, we derive the critical screening length for three bodies. As indicated in the embedded subfigure, this is $\delta_s^\circ = 2.8 \pm 0.29\ a_0$.

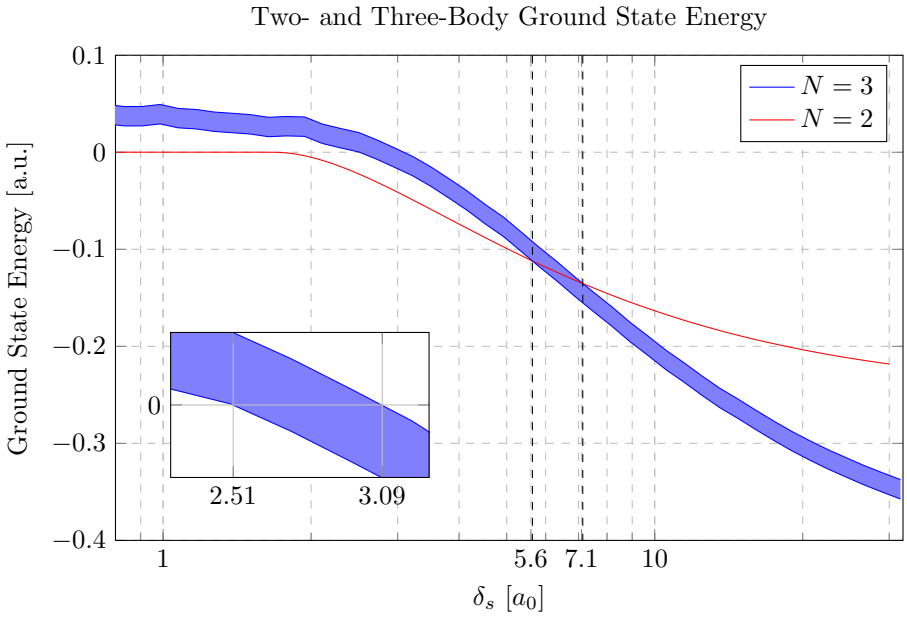

Figure 4.3: The SVM applied to three fermions of equal mass, interacting via an attractive Yukawa potential of screening length δ_s (a_0). The two-body ground state energy (red) is plotted for reference.

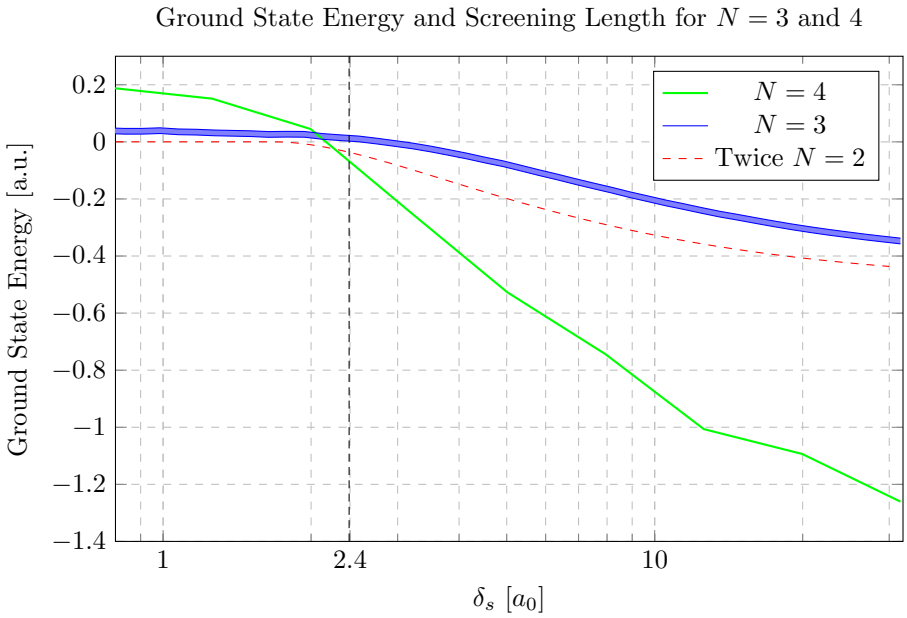

Figure 4.4: The SVM applied to three and four fermions of equal mass, interacting via an attractive Yukawa potential of screening length δ_s. The four-body result (green) is an upper bound on the ground state energy. For reference, twice the two-body ground state energy is plotted in red.

We can also determine for which values of δ_s the three-body bound state is stable or unstable. Denote the ground state energy of N particles by E_N. The only possible decay routes three bodies could take would be $3 \to 1 + 1 + 1$ or $3 \to 2 + 1$. The former is certainly not energetically favorable as long as a three-body bound state exists, whereas the latter is possible only if $E_2 < E_3$. As depicted in Figure 4.3 by the dashed lines, the unstable range is $\delta_s < 5.64\ a_0$ and the stable range is $7.14\ a_0 < \delta_s$.

We extend this analysis to include results for four fermions in Figure 4.4. This result is an upper bound; we do not assign an error estimate. Compu-

Table 4.1: Bottlenecks in Terms of δ_s (a_0).

	$0 < \delta_s < 2.39$	$2.39 < \delta_s < 5.64$	$5.64 < \delta_s < 7.14$	$7.14 < \delta_s$
$N = 3$	Unstable	Unstable	—	Stable
$N = 4$	—	Stable	Stable	Stable

tational resources were a strong limit in the four-body case, but the upper bound still allows us to derive significant conclusions. The relevant decay routes of 4 bodies are $4 \to 2 + 2$ and $4 \to 3 + 1$. The first exists when $E_4 > 2E_2$. Given that we only have an upper bound on E_4, we know this mode not to exist for $\delta_s > 2.39\ a_0$, as drawn in the figure. The second decay exists when $E_3 < E_4$, corresponding to a screening length falling in the range of the prior decay, so it may be disregarded. We calculated the δ_s that determine when the decay modes exist by interpolating the data and solving for the intersection of the corresponding interpolation functions.

We summarize our findings in Table 4.1. Interestingly, for $2.39\ a_0 < \delta_s < 5.64\ a_0$, there exists a bottleneck at $N = 3$ but not at $N = 4$. Discussing the impact of the bottlenecks indicated in Table 4.1 in terms of dark matter nucleosynthesis is beyond our scope and will be left for future work. For now, we note that we have achieved the goal of this analysis and conclude.

Chapter 5

Conclusion

The near-equal amount of normal matter and dark matter, combined with the baryonic matter asymmetry, motivates a self interaction between dark matter particles. If the interaction between the dark matter is strong enough and attractive, it is possible that the particles may form bound states analogous to nuclei. Based on this analogy, we would expect that certain configurations of N dark matter particles would be energetically preferable than others and hence decay modes may exist for certain N.

In the early universe, as nucleosynthesis was occurring among normal matter, so too it would have occurred among dark matter. A decay mode at a given N corresponds to a bottleneck in this nucleosynthesis. Bottlenecks would significantly impact the present-day distribution of dark matter. This is reinforced by the significance of the bottlenecks in normal nucleosynthesis in determining the present-day distribution of elements.

Assuming that the identical dark matter particles interact pairwise via an attractive Yukawa potential, the goal of this analysis was to understand whether bottlenecks exist given a screening length of the potential.

To this end, we sought to map the ground state energy as a function of the screening length for $N = 2, 3, 4$. The two-body case was discussed in Section 2 and gave reference to the few-body results. The transition from the two-body problem to the nontrivial few-body problem was made in Section 3. This section also gave a pedagogical overview of the concepts needed to apply the *Stochastic Variational Method* of [1], which gives an upper bound on the ground state energy of a system. The method was then applied to the example ps^-, returning upper bounds within 1% of the measured ground state energy.

In Section 4, we reported the results of applying the SVM to systems of $N = 3, 4$ equal mass fermions and compared these to the $N = 2$ case. From comparing the difference in ground state energies between $N = 2, 3, 4$ bodies, we derived the bottlenecks as given in Table 4.1.

With regards to the results of this work, the most immediate future direction of research is to apply a similar analysis with greater computational resources, both to confirm and expand upon these results. Furthermore, another method of solving the three-body problem (such as the Faddeev method) could be implemented to give more rigorous support.

Most importantly, the bottlenecks indicated in this work should be elaborated on; their full consequences should be realized in terms of the present-

day distribution of dark matter. Ultimately, this work has provided accurate results from which theory can confidently take over and predict these distributions. This is motivating: it is possible that such distributions may some day be traced by the ever-improving dark matter direct detection experiments.

Appendix A

Ritz Variational Method

In determining an upper bound on the N-body ground state energy, we employ the Ritz variational method.

The variational method is based on the identity:

$$E_0 \leq \frac{\langle \Psi | \hat{H} | \Psi \rangle}{\langle \Psi | \Psi \rangle}, \tag{A.1}$$

where E_0 is the ground state energy of the Hamiltonian $\hat{H}$. To obtain a precise upper bound of the ground state energy, we let

$$|\Psi\rangle = \sum_{i=1}^{N} c_i |\psi_i\rangle , \tag{A.2}$$

in which $\{|\psi_i\rangle\}$ is a known set of N basis functions, not necessarily orthogonal. The coefficients $\{c_i\}$ are not necessarily known. With a known $\hat{H}$, we

let

$$H_{ij} = \langle \psi_i | \hat{H} | \psi_j \rangle \qquad \text{and} \qquad B_{ij} = \langle \psi_i | \psi_j \rangle . \tag{A.3}$$

This defines H as the Hamiltonian matrix, and B as the overlap matrix. To the end of finding an upper bound, define

$$\epsilon \equiv \frac{\langle \Psi | \hat{H} | \Psi \rangle}{\langle \Psi | \Psi \rangle} = \frac{\sum_{i=1}^{N} \sum_{j=1}^{N} c_i^* c_j H_{ij}}{\sum_{i=1}^{N} \sum_{j=1}^{N} c_i^* c_j B_{ij}} \equiv \frac{C}{D}. \tag{A.4}$$

To minimize ϵ, we can proceed by minimizing via setting the partial over $\{c_i^*\}$ or $\{c_j\}$ equal to 0. We choose $\{c_i^*\}$ and evaluate the partial derivative,

$$\begin{aligned} \frac{\partial \epsilon}{\partial c_i^*} &= \frac{\sum_{j=1}^{N} c_j H_{ij}}{D} - \frac{C \sum_{j=1}^{N} c_j B_{ij}}{D^2} \\ &= \frac{\sum_{j=1}^{N} c_j H_{ij}}{D} - \epsilon \frac{\sum_{j=1}^{N} c_j B_{ij}}{D} \\ &= \frac{\sum_{j=1}^{N} c_j (H_{ij} - \epsilon B_{ij})}{D} = 0. \end{aligned}$$

This implies that

$$\sum_{j=1}^{N} c_j (H_{ij} - \epsilon B_{ij}) = 0 \qquad \text{for all} \quad i = 1, \ldots, N.$$

So that we have a set of homogeneous equations over $\{c_j\}$, which we know is consistent only if

$$\det(H - \epsilon B) = 0. \tag{A.5}$$

Solving this equation, or the corresponding generalized eigenvalue problem, will give N values of ϵ which will all be real by the fact that H and B are hermitian, and that the sum of hermitian operators is hermitian. The lowest ϵ gives the upper bound on the ground state energy.

Bibliography

[1] Y. Suzuki, Y.S.K. Varga, M. Suzuki, and K. Varga. *Stochastic Variational Approach to Quantum-Mechanical Few-Body Problems*. Number v. 54 in Lecture Notes in Physics Monographs. Springer, 1998.

[2] Mariangela Lisanti. Lectures on Dark Matter Physics. In *Proceedings, Theoretical Advanced Study Institute in Elementary Particle Physics: New Frontiers in Fields and Strings (TASI 2015): Boulder, CO, USA, June 1-26, 2015*, pages 399–446, 2017.

[3] NASA Astronomy Picture of the Day. Aug 24, 2006.

[4] V. C. Rubin, W. K. Ford, Jr., and N. Thonnard. Rotational properties of 21 SC galaxies with a large range of luminosities and radii, from NGC 4605 /R = 4kpc/ to UGC 2885 /R = 122 kpc/. *Astrophysical Journal*, 238:471–487, June 1980.

[5] Robert H. Sanders and Stacy S. McGaugh. Modified newtonian dynamics as an alternative to dark matter. *Annual Review of Astronomy and Astrophysics*, 40(1):263–317, 2002.

[6] S. Boran, S. Desai, E. O. Kahya, and R. P. Woodard. GW170817 Falsifies Dark Matter Emulators. *Phys. Rev.*, D97(4):041501, 2018.

[7] P. A. R. Ade et al. Planck 2015 results. XIII. Cosmological parameters. *Astron. Astrophys.*, 594:A13, 2016.

[8] Robert J. Scherrer and Michael S. Turner. On the Relic, Cosmic Abundance of Stable Weakly Interacting Massive Particles. *Phys. Rev.*, D33:1585, 1986. [Erratum: Phys. Rev.D34,3263(1986)].

[9] Kathryn M. Zurek. Asymmetric Dark Matter: Theories, Signatures, and Constraints. *Phys. Rept.*, 537:91–121, 2014.

[10] L.D. Landau and E.M. Lifshitz. *Quantum Mechanics: Non-Relativistic Theory*. Teoreticheskaia fizika. Elsevier Science, 2013.

[11] D. Griffiths. *Introduction to Elementary Particles*. Physics textbook. Wiley, 2008.

[12] Hideki Yukawa. On the interaction of elementary particles. i. *Proceedings of the Physico-Mathematical Society of Japan. 3rd Series*, 17:48–57, 1935.

[13] A. Zee. *Quantum Field Theory in a Nutshell: Second Edition*. In a Nutshell. Princeton University Press, 2010.

[14] John W. Norbury. The quantum mechanical few-body problem. *American Journal of Physics*, 57(3):264–266, 1989.

[15] W. Glöckle. *The Quantum Mechanical Few-Body Problem*. Theoretical and Mathematical Physics. Springer Berlin Heidelberg, 2012.

[16] J.S. Avery. *Hyperspherical Harmonics: Applications in Quantum Theory*. Reidel Texts in the Mathematical Sciences. Springer Netherlands, 2012.